A reversible and highly selective two-photon fluorescence "on-off-on" probe for biological Cu^{2+} detection

Hui Wang [a,†,*], Bin Fang[c,†], Le Zhou[a], Di Li[a], Lin Kong[c], Kajsa Uvdal,[b] Zhangjun Hu[b]

a *Department of Chemistry, Anhui provincial engineering research center for polysaccharide drugs, Wannan Medical College, Wuhu 241002, People's Republic of China*

b *Division of Molecular Surface Physics & Nanoscience, Department of Physics, Chemistry and Biology (IFM), Linköing University, 58183 Linköing, Sweden*

[c] *Department of Chemistry, Key Laboratory of Functional Inorganic Material Chemistry of Anhui Province, Anhui University, Hefei 230601, P. R. China*

† These authors contributed equally to this work and should be considered co-first authors.

E-mail address: wanghias@126.com (H. Wang)

Experimental section

1.1 Materials and apparatus

All reagents and solvents were commercially purchased, and the solvents were purified by conventional methods before using. ^{1}H-NMR and ^{13}C-NMR spectra were recorded with a Bruker Avance 400 MHz and 100 MHz spectrometer (TMS as internal standard in NMR), respectively. IR spectra (4000-400 cm^{-1}) were carried out on FT-IR spectrometer (KBr pellets). Mass spectrum was performed with a HRMS-LTQ Obritrap XL (ESI source). UV-vis absorption spectra and fluorescence spectra were carried out on UV-1700 spectrophotometer and HITACHI F-7000 fluorescence spectrophotometer, respectively. 2PA action cross-section of **L** was obtained by the two-photon excited fluorescence (2PEF) method with femtosecond laser piles and a Ti:sapphire system (680-1080 nm, 80 MHz, 140 fs) as the light source (the concentration of compound **L** was 0.5 mM).

1.2 Computational details

The calculations were carried out with the Gaussian 09 software package. The optimizations of the complex structures were performed using B3LYP density functional theory. On the basis of ground- and excited- state optimization, the TDDFT approach was applied to investigate the excited state electronic properties. The Lanl2dz basis set was used to treat the Cu atom, whereas the 6-31g* basis set was used to treat all other atoms.

1.3 Cell imaging

HepG2 cells were seeded in 24 well plates at a density of 10^5 cells per well and grown for 96 h. For live cell imaging cell cultures were incubated with compound **L** (10% PBS: 90% cell media) at concentrations 10 μM and maintained at 37 °C in an atmosphere of 5% CO_2 and 95% air for incubation times ranging for 30 min. Then, cells were washed with PBS (3×3 mL per well) and 1 mL of PBS was added to each well. The cells were imaged using confocal lasers canning microscopy and oil immersion lenses. For **L**, the excitation wavelength of 700 nm was used and the emission was measured at 520-560 nm. Co-staining was performed by incubating cells with 1 μM Hoechst 33342 (λ_{ex} = 405 nm, λ_{em} = 420–450 nm) for 15 min and 1 μM ER-Tracker (λ_{ex} = 488 nm, λ_{em} = 500–520 nm) for 30 min.

1.4 Two-photon microscopy

HepG2 cells were luminescent imaged on a Zeiss LSM 710 META confocal laser scanning microscope using magnification 63×oil-dipping lenses for monolayer cultures. Image data acquisition and processing were performed using Zeiss LSM Image Browser, Zeiss LSM Image Expert and Image J.

1.5 MTT assay

To ascertain the cytotoxic effect of **L** treatment over a 24 h period, the 5-dimethylthiazol-2-yl-2,5-diphenyltetrazolium bromide (MTT) assay was performed. HepG2 cells were grown to ~85 % confluence in 96-well plates before treatment. Prior to the compounds' treatment, the growth medium was refreshed, and **L** was first dissolved in DMSO to 1 mM and then diluted twice by DMEM cell culture medium to obtain the final concentrations. The treated cells were incubated for 24 h at 37 °C and under 5% CO_2. Subsequently, the cells were treated with 5 mg/mL MTT solution (10 μL/well) and incubated for an additional 4 h (37 °C, 5% CO_2). Then, MTT solution was removed and the formazan crystals were dissolved in DMSO (100 μL/well). The absorbance at 490 nm was recorded. Three independent trials were conducted, and the averages and standard deviations are plotted. The reported cell survival percent are relative to untreated control cells.

1.6 Association constant calculation

The association constants between **L** and Cu^{2+} were analyzed using the fluorescence data and were calculated employing Benesi-Hildebrand:

$$1/(F_0-F)=1/(K_a(F_0-F_{min})[Cu^{2+}])+1/(F_0-F_{min})$$

where F and F_0 represent the fluorescence emission of **L** in the presence and absence of Cu^{2+}, respectively, F_{min} is the saturated emission of **L** in the presence of excess amount of Cu^{2+}. $[Cu^{2+}]$ is the concentration of Cu^{2+} added, and K_a is the binding constant.

1.7 Job-plot's equation

$C_M+C_R=C^0$, where C_0 is a constant, the concentration of L and Cu^{2+} is C_M and C_R, respectively.

$$f_M=C_M/(C_M+C_R)$$

$$f_R=C_R/(C_M+C_R)$$

where *f* is the mole fraction. When the ratio of the molar fraction of the metal ion and the ligand reaches the maximum, the corresponding number is the coordination number.

Table S1. Crystal data collection and structure refinement of **L**.

Compound	**L**
Empirical formula	$C_{21}H_{29}N_3O_3$
CCDC	1547404
Formula weight	371.47
Crystal system, space group	Orthorhombic, Pbca
Unit cell dimensions(Å)	a=16.772(3)
	b= 9.064(2)
	c=25.832(4)
Volume/ Å^3	3926(1)
Z, Calculated density/Mg m^3	8, 1.257
Absorption coefficient/mm^{-1}	0.085
F(000)	1600
Theta range for data collection/	1.577 to 18.305
Goodness-of-fit on F^2	1.012
Final R indices [I□2σ]	R1=0.0365, wR2=0.0965
Large diff. peak and hole/e Å^{-3}	0.189 and -0.110

Table S2. Selected bond lengths (Å) and angles (°) of **L**.

L			
N(2)-C(11)	1.282(4)	C(11)-N(2)-C(12)	126.3(3)
N(2)-C(12)	1.417(4)	C(5)-N(1)-C(2)	121.2(3)
C(8)-C(11)	1.440(5)	C(13)-C(12)-N(2)	126.9(4)

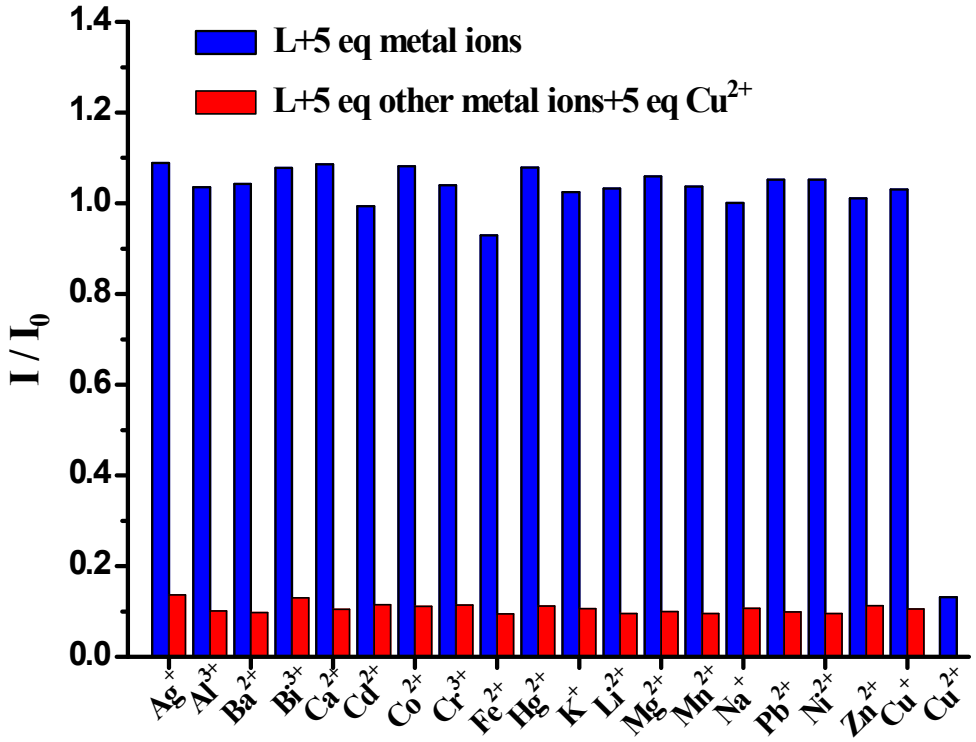

Figure S1 The selectivity of **L** (12.5 μM) in ethanol/HEPES buffer (pH=7.42) (v/v, 1:1). The blue bars represent the fluorescence intensity after addition of various ions (5 equiv.). The red bars represent the fluorescence intensity that occurs upon the subsequent addition of Cu^{2+} (5 equiv.) to the above solution (λ_{ex} = 440 nm).

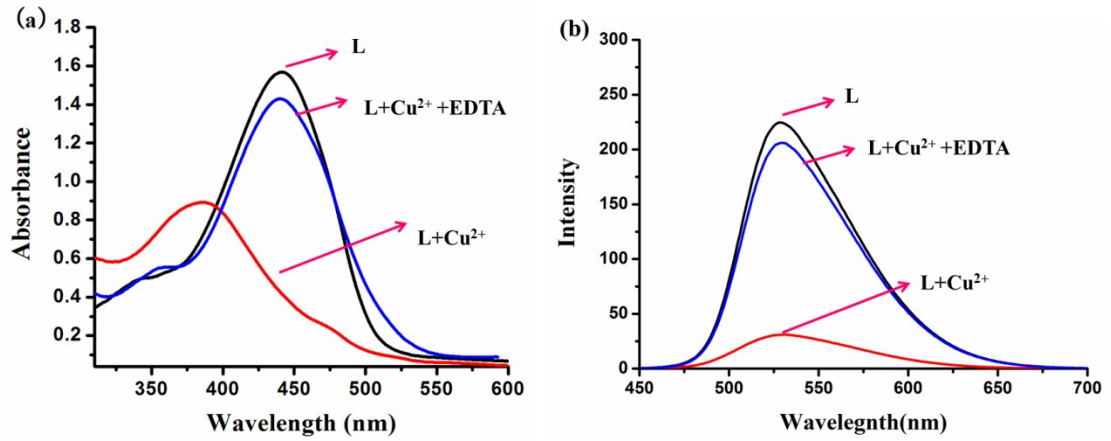

Figure S2 (a) UV-vis absorption and (b) fluorescence spectra of **L** (12.5 μM) before and after the addition of Cu^{2+} (2 equiv) and EDTA (2.5 equiv), respectively, in ethanol/HEPES buffer (pH=7.42) (v/v, 1:1).

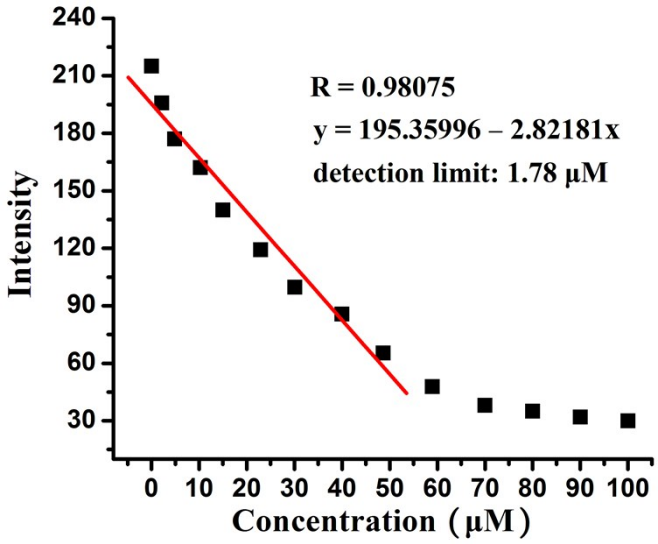

Figure S3 The limit of detection (LOD) of **L** for Cu^{2+}: fluorescence responses as a function of Cu^{2+} concentration. The solid line represents a linear fit to the experimental data.

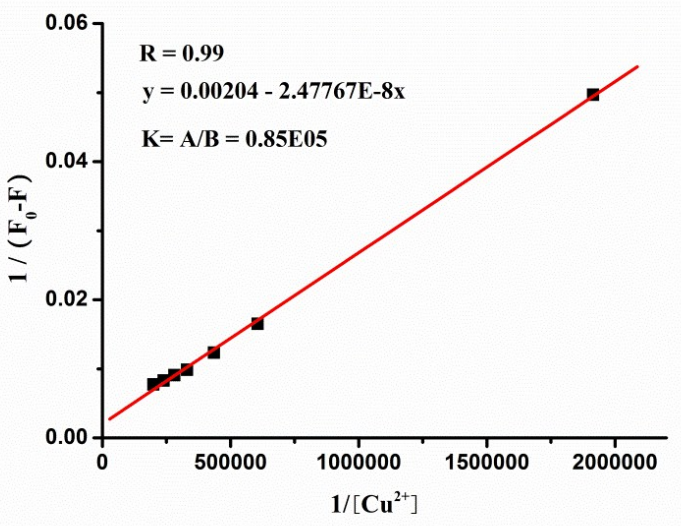

Figure S4 Benesi-Hildebrand plot for **L** towards Cu^{2+} in ethanol/HEPES buffer (pH=7.42) (v/v, 1:1).

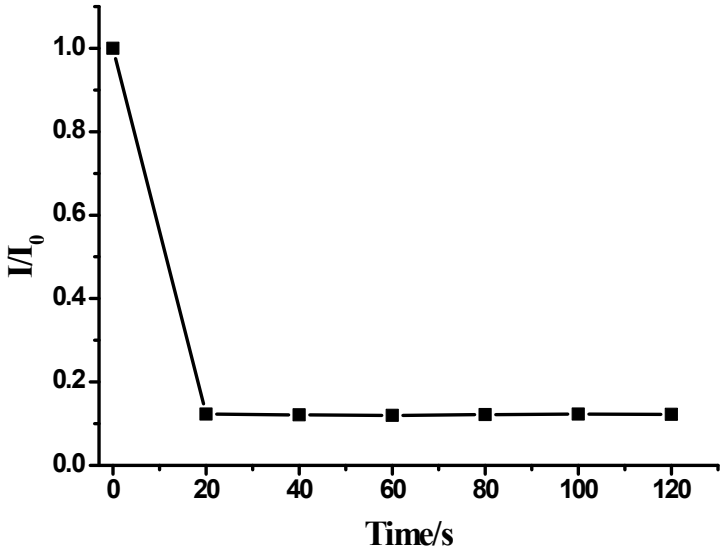

Figure S5 Relatively fluorescence intensity of **L** (12.5 μM) vs. the reaction time in the presence of 1 equiv. Cu^{2+} in ethanol/HEPES buffer (pH=7.42) (v/v, 1:1).

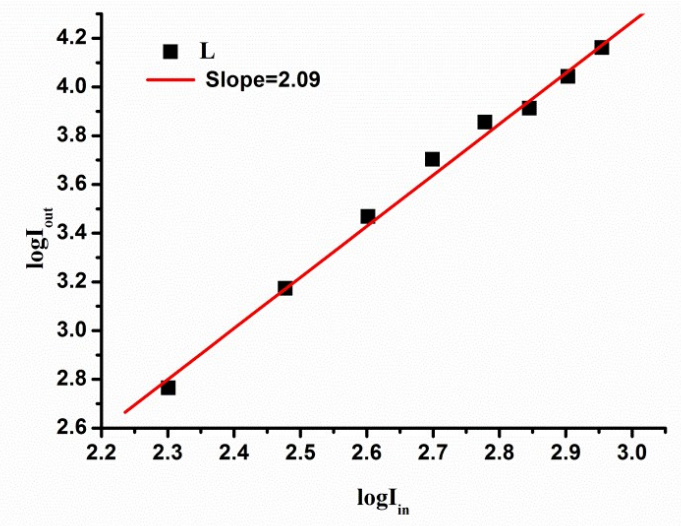

Figure S6 Output fluorescence (I_{out}) vs. the square of input laser power (I_{in}) for **L**.

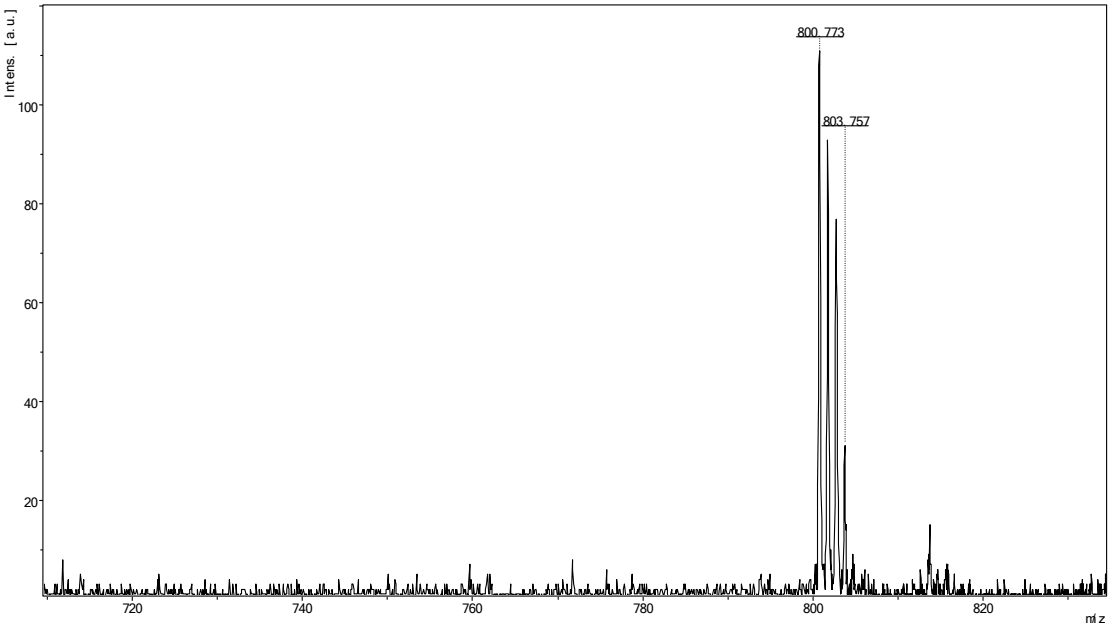

Figure S7 MS spectra of **LCu**.

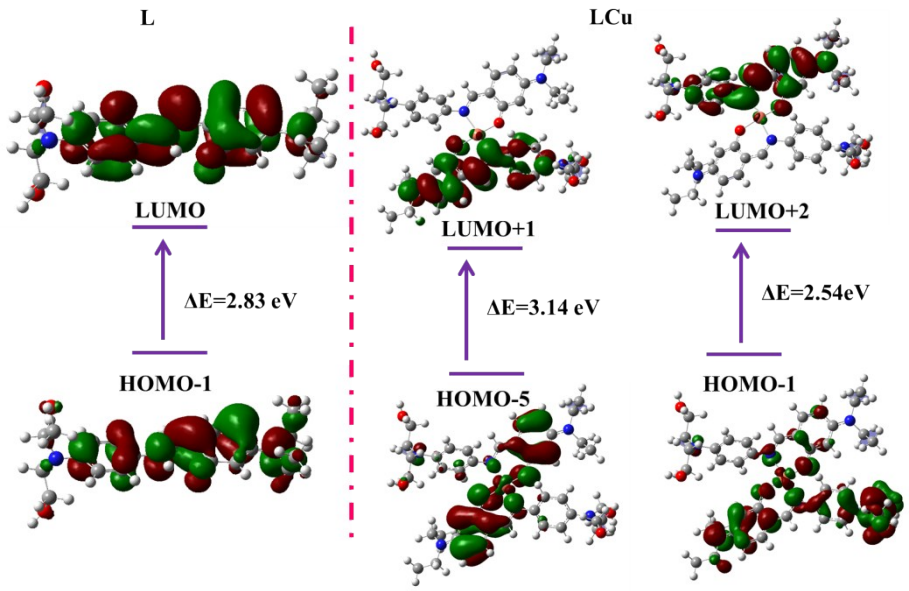

Figure S8 The frontier molecular orbitals distributions of **L** and **LCu**.

Table S3 Calculated leaner absorption properties (nm), excitation energy (eV), oscillator strengths and major contribution for **L** and **LCu**.

Compound	ΔE_1[a]	λ[nm][b]	Oscillator strengths	Nature of the transition
L	2.83	437	1.224	99(H-1)→101(L)(0.68)
LCu	2.54	488	0.0620	207(H-1)→211(L+2)(0.62)
	3.14	394	0.2502	203(H-5)→210(L+1)(0.52)

[a] The energy gap of the single-photon absorption band. [b] Peak position of the maximum absorption band.

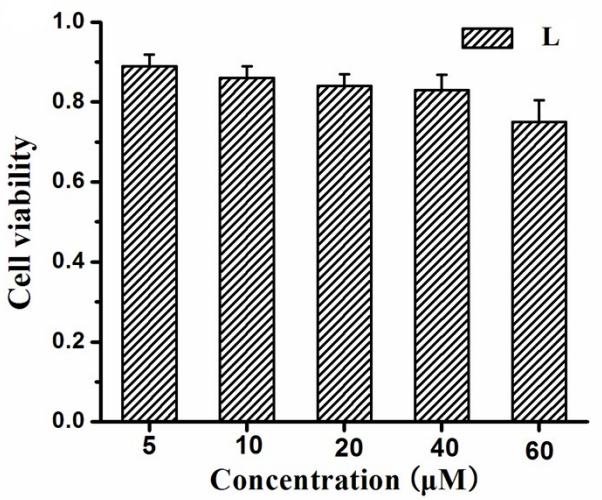

Figure S9 Cytotoxicity data results obtained from the MTT assay treated with **L** at di□erent concentrations for 24 h, respectively.

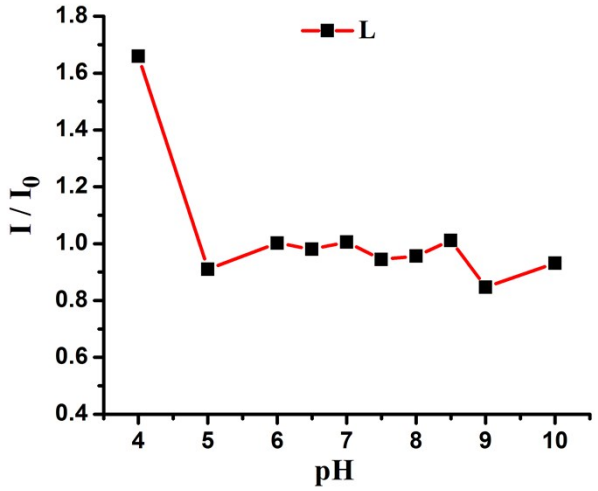

Figure S10 The changes of emission intensity of **L** (10 μM) in HEPES buffer at various pH.

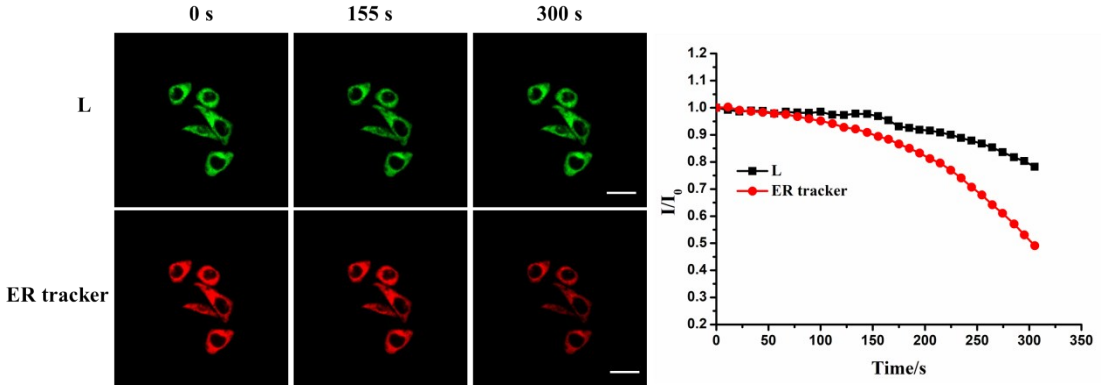

Figure S11 Photobleaching experiment of **L** in HepG2 cells. (left) Confocal fluorescence images of live HepG2 cells stained with **L** or ER tracker. (right) Relative intensity loss of fluorescence emission of **L** and ER tracker with an increasing bleaching time. Scale bar = 20 μm.

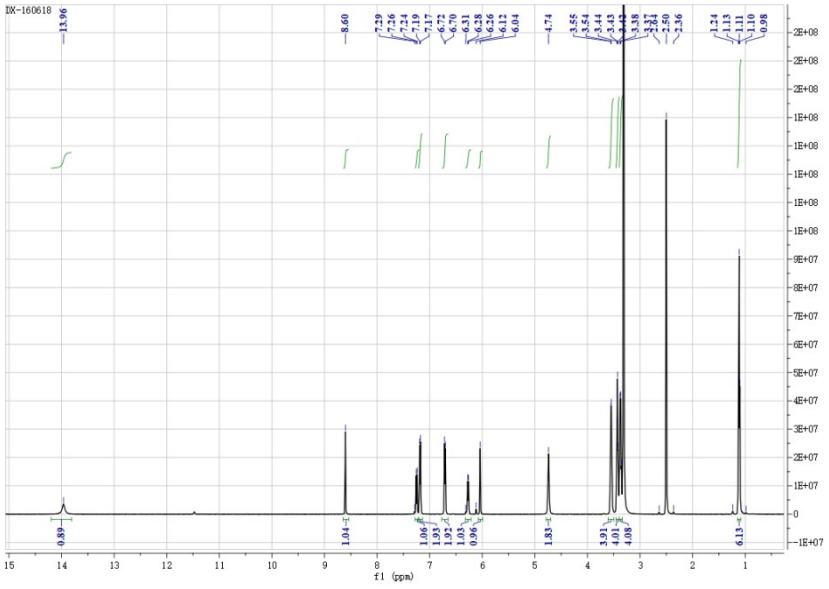

Figure S12 ^{1}H NMR spectra of **L**.

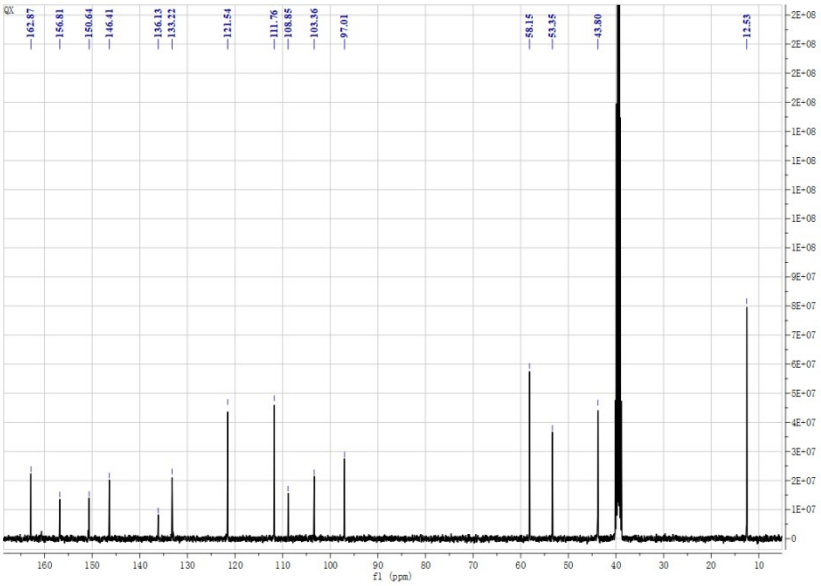

Figure S13 ^{13}C NMR spectra of **L**.

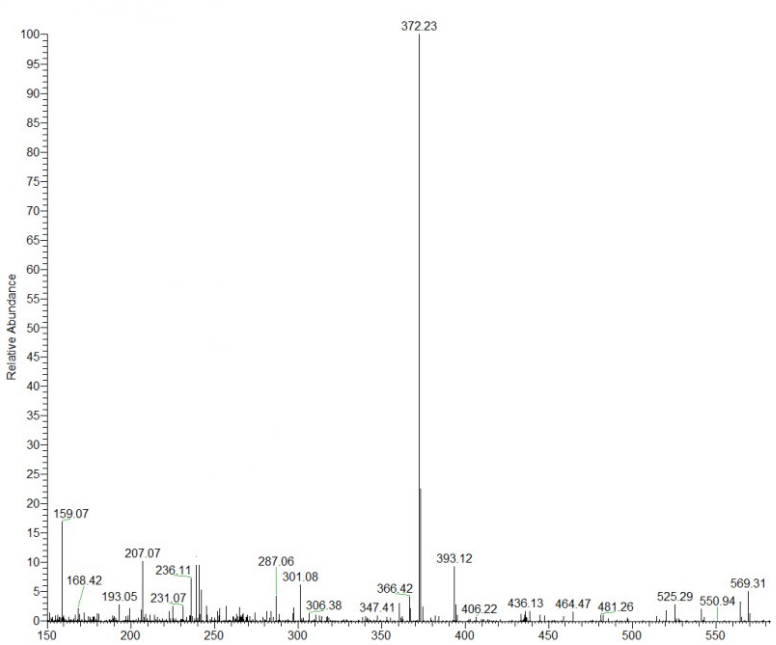

Figure S14 ESI-MS spectra of **L**.

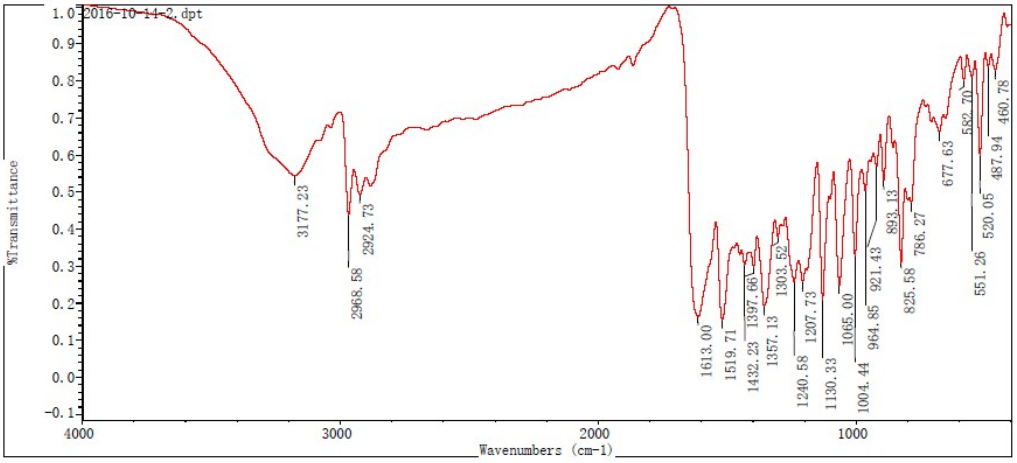

Figure S15 FT-IR spectra of **L**.